On the origin of the soft photons of the high synchrotron peaked blazar : PKS 1424+240

Shi-Ju Kang[1,2]⋆, Yong-Gang Zheng[3], Qingwen Wu[2]⋆† and Liang Chen[4]

[1] *Department of Physics and Electronics Science, Liupanshui Normal University, Liupanshui, Guizhou, 553004, China*
[2] *School of Physics, Huazhong University of Science and Technology, Wuhan, Hubei, 430074, China*
[3] *Department of Physics, Yunnan Normal University, Kunming, Yunnan, 650092, China*
[4] *Key Laboratory for Research in Galaxies and Cosmology, Shanghai Astronomical Observatory*
 Chinese Academy of Sciences, 80 Nandan Road, Shanghai, 200030, China

ABSTRACT
PKS 1424+240 is a distant very high energy gamma-ray BL Lac object with redshift $z = 0.601$. It was found that pure synchrotron self-Compton (SSC) process normally need extreme input parameters (e.g., very low magnetic field intensity and extraordinarily large Doppler factor) to explain its multi-wavelength spectral energy distributions (SEDs). To avoid the extreme model parameters, different models have been proposed (e.g., two-zone SSC model or lepto-hadronic model). In this work, we employ the traditional one-zone leptonic model after including a weak external Compton component to re-explore the simultaneous multi-wavelength SEDs of PKS 1424+240 in both high (2009) and low (2013) states. We find that the input parameters of magnetic field and Doppler factor are roughly consistent with those of other BL Lacs if a weak external photon field from either broad line region (BLR) or the dust torus. However, the required energy density of seed photons from BLR or torus is about 3 orders of magnitude less than that constrained in luminous quasars (e.g., flat-spectrum radio quasars, FSRQs). This result suggests that the BLR/torus in BL Lacs is much weaker than that of luminous FSRQs (but not fully disappear), and the inverse-Compton of external photons from BLR/torus may still play a role even in high synchrotron peaked blazars.

Key words: BL Lacertae objects: individual (PKS 1424+240, VER J1427+23)

1 INTRODUCTION

Blazars, including flat-spectrum radio quasars (FSRQs) and BL Lacertae objects (BL Lacs), are radio-loud active galactic nuclei (AGNs) with a relativistic jet pointed at a small viewing angle to the line of sight. The multi-wavelength spectral energy distributions (SEDs) from the radio to the γ-ray bands of blazars dominantly come from the non-thermal emission, where the SED normally exhibits a two-hump structure in the $\nu - \nu F_\nu$ space. The lower energy hump is normally attributed to the synchrotron emission produced by the non-thermal electrons in the jet while the second hump mainly come from inverse Compton (IC) scattering. The seed photons for IC scattering may come from the synchrotron photons (SSC process, e.g., Konigl 1981; Marscher & Gear 1985;

Ghisellini & Maraschi 1989) and/or external photons (EC process), where the external photons possibly originate from the accretion disk (e.g.,Dermer & Schlickeiser 1993; Böttcher, Mause & Schlickeiser 1997), the broad line region (BLR; e.g., Sikora et al. 1994; Ghisellini & Madau 1996), and/or the molecular torus (e.g., Błażejowski et al. 2000; Ghisellini & Tavecchio 2008).

PKS 1424+240 (VER J1427+237) is possibly the most distant BL Lac object (or the third most distant blazar) with a redshift of $z = 0.6010 \pm 0.003$ (Rovero et al. 2016) that detected the very high energy (VHE; $E \geqslant 100$ GeV) γ-ray emission up to now. The other two VHE blazars are FSRQs (S3 0218+357, $z = 0.944 \pm 0.002$, Cohen et al. 2003, Mirzoyan 2014, Sitarek et al. 2015 and PKS 1441+25, $z = 0.9397 \pm 0.0003$, Shaw et al. 2012; Mirzoyan 2015). PKS 1424+240 was first observed in the radio band (408 MHz) in the 1970s (Fanti et al. 1974), and was categorized as a blazar based on its optical polarization (Impey & Tapia 1988 and Fleming et al. 1993). Based on its weak emission-line fea-

---

⋆ E-mail: kangshiju@hust.edu.cn
† Corresponding author: qwwu@hust.edu.cn

ture and the peak frequency of the lower energy bump, PKS 1424+240 is categorized as an intermediate-energy-peaked BL Lac (IBL) (Nieppola et al. 2006), or a high-energy-peaked BL Lac (HBL) (Padovani & Giommi 1996). PKS 1424+240 was most recently classified as a high synchrotron peaked (HSP, which is the commonly utilized categorization now; Abdo et al. 2010) BL Lac object in Archambault et al. (2014).

PKS 1424+240 was detected in γ-rays by the Fermi Large Area Telescope (LAT; Atwood et al. 2009) with a very hard spectrum (photon index $\Gamma = 1.85 \pm 0.07$, Abdo et al. 2009). The VHE γ-ray emission was also detected in Spring of 2009 by VERITAS (Ong 2009) and confirmed as a VHE emitter by MAGIC (Teshima 2009). Different models have been proposed to explain its hard VHE γ-ray spectrum. One-zone SSC model normally require a very large Doppler facotor of $\delta \sim 50 - 130$ and a quite weak magnetic field of ~ 0.02 G (e.g., Acciari et al. 2010, Aleksić et al. 2014). To overcome these extreme parameters, Aleksić et al. (2014) proposed a two-zone SSC model and found that it can roughly describe multi-wavelength SED of PKS 1424+240 with reasonable model parameters. Yan & Zhang (2015) suggested that the extreme model parameters can also be avoided if adopting a lepto-hadronic hybrid jet model, where the VHE γ-ray emission is attributed to the synchrotron emission of pair cascades resulting from $p\gamma$ interaction (Yan et al. 2015).

Some recent works found that it can overcome the extreme parameters in a few BL Lacs if including a weak EC component (Acciari et al. 2008; Abdo et al. 2011a; Prandini et al. 2012; Liao et al. 2013; Liao et al. 2014). To understand the VHE emission in the most distant BL Lac of PKS 1424+240, we try to explore whether the traditional one-zone leptonic model after including a weak EC component can explain its multi-wavelength SED or not. Throughout the letter, we assume the following cosmology: $H_0 = 70$ km s^{-1}Mpc^{-1}, $\Omega_0 = 0.3$ and $\Omega_\Lambda = 0.7$.

2   THE MODEL

In this work, we adopt the traditional one-zone synchrotron + IC model to fit the SEDs of PKS 1424+240, which is widely used in blazars (see e.g., Ghisellini et al. 2010, and references therein). A homogeneous sphere with radius R embedded in a magnetic field B is assumed, that moves relativistically with a speed of $\upsilon = \beta c$ (bulk Lorentz factor $\Gamma = 1/\sqrt{1 - \beta^2}$) along the jet orientation. Doppler factor $\delta = [\Gamma (1 - \beta \cos \theta)]^{-1} \approx \Gamma$ is assumed for the relativistic jet with a small viewing angle $\theta \leqslant 1/\Gamma$. The electron spectrum is assumed as a broken power-law distribution, with indices p_1 and p_2 below and above the break energy $\gamma_b m_e c^2$,

$$N(\gamma) = \begin{cases} N_0 \gamma^{-p_1} & \gamma_{\min} \leqslant \gamma \leqslant \gamma_{\rm b} \\ N_0 \gamma_{\rm b}^{p_2 - p_1} \gamma^{-p_2} & \gamma_{\rm b} < \gamma \leqslant \gamma_{\max} \end{cases} \quad (1)$$

where $\gamma_{\min}$ and $\gamma_{\max}$ are the minimum and maximum electron Lorentz factors, and N_0 is the normalization of the particle distribution. Such a broken power-law distribution is a steady-state electron spectrum, which could be the result of the balance between the particle cooling and escape rates in the blob (e.g., Kardashev 1962; Sikora et al. 1994; Inoue & Takahara 1996; Kirk et al. 1998;

Ghisellini et al. 1998; Böttcher & Chiang 2002; Chen et al. 2012; Böttcher et al. 2013).

Different from the FSRQs, we consider a possible weaker external Compton process (e.g., external photons from BLR or torus) in this HSP BL Lac, where the external seed photon field may still play some roles in Compton process in some BL Lacs (e.g., Böttcher et al. 2002; Böttcher & Chiang 2002). Since the location of the γ-ray emission region is still unclear, we assume the external seed photons predominantly originate either from the BLR or from the dust torus. The external radiation field is characterized by an isotropic blackbody with the temperature $T = h\nu_{\rm p}/(3.93k_B)$, where $\nu_{\rm p}$ is the peak frequency of seed photons in the $\nu - \nu F_\nu$ space. For the BLR cloud, the most prominent contribution comes from the Lyα line, and hence the spectrum is assumed to be a blackbody with a peak around 2×10^{15} Γ Hz (see, Ghisellini & Tavecchio 2008). For the IR torus, the spectrum is assumed to be a blackbody with a peak frequency of $\nu_{\rm IR} = 3 \times 10^{13}$ Γ Hz in the comoving frame (Cleary et al. 2007). The Klein-Nishina effect in the inverse Compton scattering and the self-absorption effect in synchrotron emission are properly considered (see, Rybicki & Lightman 1979; Blumenthal & Gould 1970).

PKS 1424+240 is a distant VHE blazar and the VHE emission is expected to be significantly absorbed by the extragalactic background light (EBL) via pair production. The absorption of gamma-rays by the EBL can be estimated using the model-dependent gamma-ray opacity of $\tau(\nu, z)$, where the relation between the observed spectrum, $F_{\rm obs}(\nu)$, and the intrinsic spectrum, $F_{\rm in}(\nu)$, can be described by the following relation,

$$F_{\rm obs}(\nu, z) = e^{-\tau(\nu, z)} F_{\rm in}(\nu, z), \quad (2)$$

where $\tau(\nu, z)$ is the absorption optical depth due to interactions with the EBL (Kneiske et al. 2004; Dwek & Krennrich 2005; Gilmore et al. 2012; Franceschini et al. 2008; Finke et al. 2010; Kneiske & Dole 2010; Domínguez et al. 2011; Ackermann et al. 2012; Abramowski et al. 2013). In order to minimize hardening introduced from EBL absorption corrections, we adopt the absorption optical depth that derived from the EBL model proposed by Domínguez et al. (2011) in our calculations. In our SED modeling of Figure 1, we assume the model prediction as the intrinsic emission and correct it to our local universe using equation (2), and compare it with the observational data (e.g., Zheng & Zhang 2011; Zheng & Kang 2013; Zheng et al. 2013, 2014; Kang et al. 2014).

3   MODELING THE SEDS OF PKS 1424+240

The simultaneous multi-wavelength data from VHE (VERITAS), HE (*Fermi*) γ-ray, X-ray and UV (*Swift*) for PKS 1424+240 at two different states are collected, where the high state in 2009 and low state in 2013 have integral flux above 120 GeV around $(2.1 \pm 0.3) \times 10^{-7}$ph m^{-2} s^{-1} and $(1.02 \pm 0.08) \times 10^{-7}$ph m^{-2} s^{-1}, respectively (see Archambault et al. 2014 for more details on the multi-waveband data). In Figure 1, the red solid points represent the simultaneous observational data (in 2009 and in 2013), empty blue squares indicate the extended LAT data set (MJD 54682 to 56452; see Archambault et al. 2014). The

non-simultaneous radio to sub-millimeter data (30 GHz to 857 GHz) from Plank were also plotted (blue solid square, the down triangles represent the upper limits, Giommi et al. 2012).

We apply the one-zone jet model as described in Section 2 to reproduce the multi-waveband SEDs of PKS 1424+240. There are 9 and 10 parameters in the pure SSC and SSC+EC models respectively: R, δ, B, p_1, p_2, $\gamma_{\min}$, $\gamma_{\max}$, $\gamma_{\rm b}$, N_0 and $U_{\rm ext}$ (energy density of external photon fields of BLR or IR). In order to reduce the number of free parameters, the radius of the emitting region in jet frame can be constrained from the minimum variability timescale and redshift with $R \leqslant \delta \Delta t / (1+z) \sim 1.6 \times 10^{15}\delta$ cm, where X-ray variability timescale of ~ 1 day (Aleksić et al. 2014) is adopted. The index of electron spectrum, p_2, is derived from the fitting the observational X-ray spectrum with a power-law function ($F_\nu \propto \nu^{-\alpha}$, $p_2 = 1 + 2\alpha$, e.g., Zhang et al. 2012, 2014), where the best-fit values of p_2 are 4.12 and 5.07 for data of 2009 and 2013 respectively. The typical $\gamma_{\min} = 40$ (e.g., Zhang et al. 2014; Kang et al. 2014) and $\gamma_{\max} = 1 \times 10^8$ ($\gamma_{\max} >> 100\gamma_{\rm b}$) are adopted in our fitting, which will not affect our main results. The other parameters B, δ, p_1, $\gamma_{\rm b}$, N_0 or/and $U_{\rm ext}$ keep free in our fitting.

The multi-wavelength SEDs of PKS 1424+240 are reproduced using the least-square (χ^2) fitting technique (e.g. Mankuzhiyil et al. 2011; Zhang et al. 2012, 2014; Kang et al. 2014). Similar to Aleksić et al. (2014), the non-simultaneous radio data (the blue filled square in Figure 1) is also included in χ^2 fitting, due to a possible correlation between radio and optical emission which suggest a common origin of the two bands emission (Aleksić et al. 2014). There are 29 observational data points (28 simultaneous UV, X-ray and γ-ray data) in the high state (2009) and 28 observational data points (27 simultaneous UV, X-ray and γ-ray data) in the low state (2013) in the SED modeling. In χ^2 fitting, we consider the observational error of the data points in the radio, X-ray and γ-ray band. For the UV data with no reported uncertainties, we take 2% of the observational flux as the error (e.g., Zhang et al. 2012; Aleksić et al. 2014). We generate all the parameters in a broad range, and calculate the reduced $\chi_{\rm r}^2$ for these parameters. Then we derive the probability distribution of $\chi_{\rm r}^2$ (e.g., $p \propto \exp(-\chi_{\rm r}^2)$), and the maximum probability corresponds the best-fit parameters. The 1σ uncertainty of each parameter is derived from the Gaussian fit to its probability distribution by setting other parameter to its best-fit value (e.g., Zhang et al. 2012, 2014; Kang et al. 2014).

The best fits are shown in Figure 1. The dotted, dashed, dot-dashed and solid lines represent the synchrotron, SSC, EC and total emission respectively. The left column and right column show the SEDs of high state in 2009 and low state in 2013 respectively, where the upper, middle and lower panels correspond to the fitting result using different models (EC-BLR, EC-IR and pure SSC). The best-fit parameters, uncertainties and the values of χ^2 are listed in Table 1. We find that the SEDs of the high state (2009) and the low state (2013) can roughly be reproduced by the leptonic jet model with pure SSC, EC-IR and EC-BLR models respectively. Similar to former works (e.g., Acciari et al. 2008; Abdo et al. 2011a; Aleksić et al. 2012; Prandini et al. 2012; Liao et al. 2013; Liao et al. 2014), the quite weak magnetic field and extraordinarily large Doppler factor are needed in

the pure SSC model, where $B = 0.02$ G, $\delta = 51.47$ in low state of 2013 and $B = 0.05$ G, $\delta = 40.23$ in high state of 2009. After considering possible EC component (either IR or BLR seed photons), we find that the model parameters are quite match with those of other BL Lacs, where $B = 0.1 - 0.3$ G and $\delta = 25 - 30$ in both states. We note that the energy density of BLR or IR in our modeling is much lower than that of luminous FSRQs, where $U_{\rm ext,BLR} = (3.71 \pm 0.65) \times 10^{-5}$ erg cm^{-3} (high state of 2009), $U_{\rm ext,BLR} = (1.62 \pm 0.48) \times 10^{-5}$ erg cm^{-3} (low state of 2013) and $U_{\rm ext,IR} = (8.24 \pm 0.33) \times 10^{-7}$ erg cm^{-3} (high state of 2009), $U_{\rm ext,IR} = (4.09 \pm 0.37) \times 10^{-7}$ erg cm^{-3} (low state of 2013) in rest frame.

4 CONCLUSION AND DISCUSSION

In this work, we employ a leptonic model with the least-square (χ^2) fitting technique to reproduce the multi-wavelength SED of PKS 1424+240 in both high (2009) and low (2013) states. Both pure SSC and SSC+EC process are considered in our model even this source is a BL Lac object. After including a weak EC component, we find that the model parameters are quite reasonable as in most of other BL Lacs while extreme model parameters are needed in pure SSC process. We propose that BLR and/or IR torus may become weak (but not fully disappear) and still play a role in external Compton scattering of low-power BL Lacs.

Pure SSC model was widely adopted in fitting the multi-wavelength SED of HBL BL Lacs (e.g., Mastichiadis & Kirk 1997; Krawczynski et al. 2004; Zhang et al. 2014), while luminous FSRQs prefer SSC+EC model (e.g., Sambruna et al. 1999; Chen & Bai 2011; Yan et al. 2014). Böttcher & Chiang (2002) proposed that the EC from BLR may play a role in some intermediate and low-energy-peaked BL lacs. For HSP PKS 1424+240, in our modeling, both pure SSC and SSC+EC process are considered to model the multi-wavelength SED in both high (2009) and low (2013) states. Nonetheless, the extreme parameters are needed if the pure SSC model is adopted for PKS 1424+240, where the magnetic field is quite low and the Doppler factor is extraordinarily large. This phenomenon is consistent with several other BL Lacs that pure SSC normally need extreme input parameters (e.g., Acciari et al. 2008; Abdo et al. 2011a; Abdo et al. 2011b; Aleksić et al. 2012; Aliu et al. 2012; Prandini et al. 2012; Liao et al. 2013; Rani et al. 2013; Liao et al. 2014). After including a weak external photon field, both the magnetic field intensity and Doppler factor are roughly consistent with most of other BL Lacs, where the average values of magnetic field strength $B \sim 0.3$ G and Doppler factor $\delta \sim$ 10-20 (see Zhang et al. 2012; Ghisellini et al. 2014). After considering a weak EC component, the ratio of magnetic energy and emitting-electron energy in the blob $\epsilon_B = L_B/L_{\rm e} \sim 1$ is also quite consistent with other BL Lacs (e.g., Ghisellini et al. 2014), while its value is < 0.1 in SSC model. So, the extreme input model parameters of pure SSC process in both states suggest that the EC process may play a role in PKS 1424+240 even we cannot fully exclude that this source do has some kind of extreme physical properties compared other BL Lacs. It should be noted that the two-zone jet model and lepto-hadronic jet
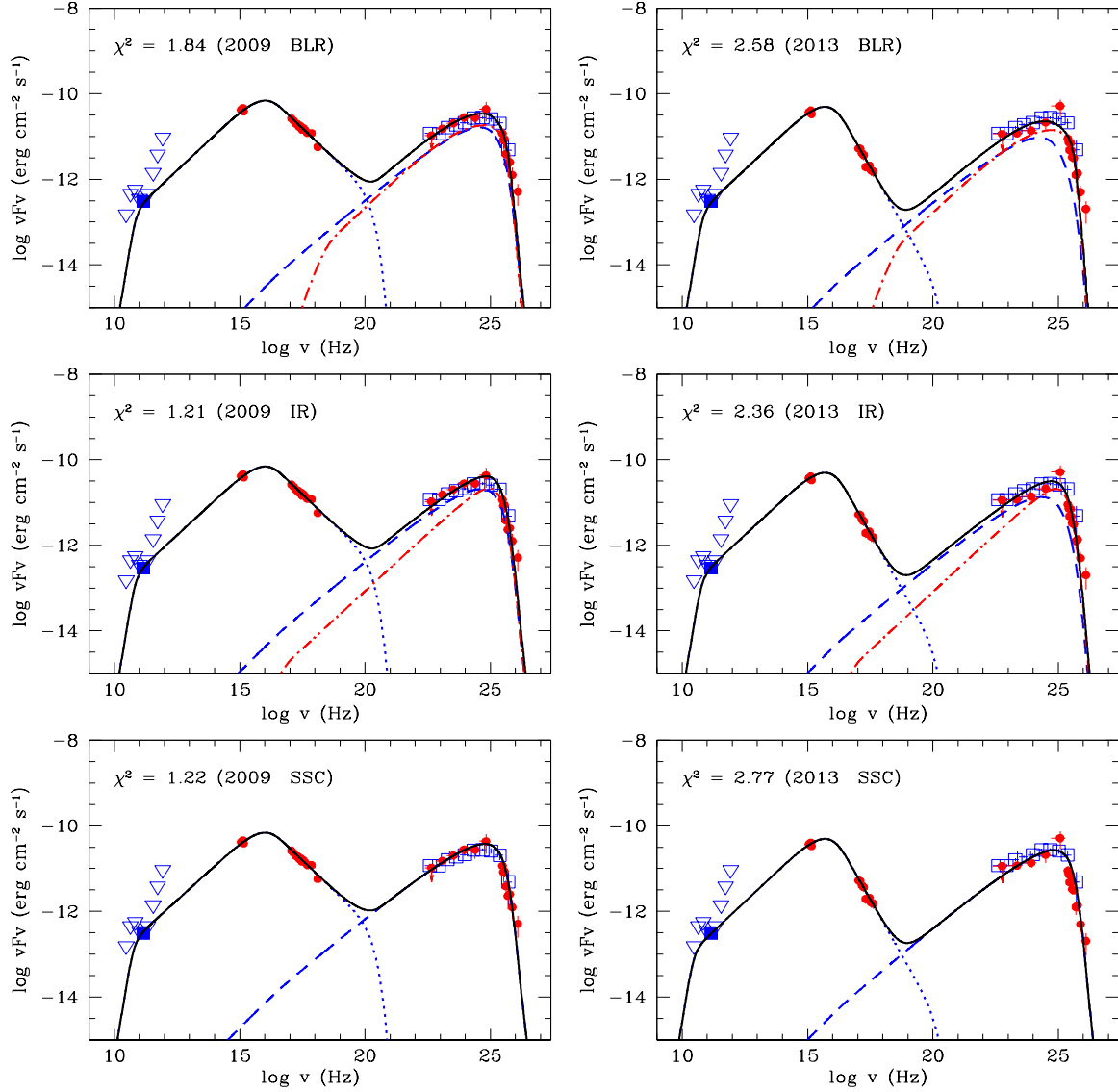
Figure 1. The SEDs of PKS 1424+240. The red solid points represent the broadband simultaneous observational data, empty blue squares indicate extended LAT data set (MJD 54682 to 56452), the non-simultaneous radio to submm data from Plank (30 GHz to 857 GHz) are also plotted (blue triangles represent the upper limit, see (Giommi et al. 2012). The dotted, dashed, dot-dashed and solid lines represent the synchrotron, SSC, EC and total emission respectively. The left column and right column show the SEDs of high state in 2009 and low state in 2013 respectively, while the upper, middle, and lower panels correspond to the fitting result using different models (EC-BLR, EC-IR and SSC).

Table 1. The relevant parameters of PKS 1424+240 (input model parameters and output luminosities).

| Model | high state(2009) | | | low state(2013) | | |
Parameter	(BLR)	(IR)	(SSC)	(BLR)	(IR)	(SSC)
B (G)	0.26 ± 0.11	0.20 ± 0.04	(0.52 ± 0.04)e-1	0.20 ± 0.03	0.14 ± 0.04	(0.22 ± 0.02)e-1
δ	27.28 ± 2.32	28.51 ± 2.67	40.23 ± 2.71	29.81 ± 2.89	31.58 ± 2.53	51.47 ± 4.47
p_1	1.91 ± 0.03	1.92 ± 0.04	1.93 ± 0.03	1.90 ± 0.04	1.91 ± 0.02	1.90 ± 0.05
$\gamma_b(10^4)$	2.45 ± 0.37	2.71 ± 0.43	4.52 ± 0.33	2.11 ± 0.46	2.44 ± 0.29	4.80 ± 0.42
$N_0(\mathrm{cm}^{-3})$	80.96 ± 31.74	107.77 ± 34.55	99.87 ± 14.63	69.91 ± 21.25	88.51 ± 19.69	49.41 ± 9.27
$U_{\mathrm{ext}}(10^{-5}\mathrm{erg\ cm}^{-3})$	3.71 ± 0.65	(8.24 ± 0.33)e-2	...	1.62 ± 0.48	(4.09 ± 0.37)e-2	...
χ_{r}^2	1.84	1.21	1.22	2.58	2.36	2.77
$L_B(\mathrm{erg\ s}^{-1})$	9.42×10^{44}	6.76×10^{44}	1.74×10^{44}	7.93×10^{44}	4.97×10^{44}	8.80×10^{44}
$L_{\mathrm{e}}(\mathrm{erg\ s}^{-1})$	4.35×10^{44}	6.19×10^{44}	2.22×10^{45}	5.12×10^{44}	7.86×10^{44}	3.63×10^{45}
$\epsilon_B = L_B/L_{\mathrm{e}}$	2.16	1.09	0.078	1.55	0.63	0.024

model are also adopted to avoid the extreme jet parameter in this source (Aleksić et al. 2014,Yan & Zhang 2015), and both of them can give a reasonable fit without the extreme model parameters. Future multi-wavelength variations and better multi-wavelength SED may help to further test this issue.

The input energy density of external photon fields $U_{\rm BLR} \sim (1-4) \times 10^{-5}$ erg cm^{-3} or $U_{\rm IR} \sim (4-8) \times 10^{-7}$ erg cm^{-3} in low and high state are about 3 orders of magnitude lower than that in luminous FSRQs, where $U_{\rm BLR} \sim 2.6 \times 10^{-2}$ erg cm^{-3} (see Ghisellini & Tavecchio 2008; Ghisellini & Tavecchio 2009, for details) and $U_{\rm IR} \sim 3 \times 10^{-4}$ erg cm^{-3} (see Ghisellini & Tavecchio 2008; Cleary et al. 2007, for details). It should be noted that the required low external seed photon field in PKS 1424+240 is also roughly consistent with those of several other BL Lacs (e.g., Acciari et al. 2008; Abdo et al. 2011a; Abdo et al. 2011b; Aliu et al. 2012; Prandini et al. 2012; Liao et al. 2013; Liao et al. 2014). The physical reason for this low seed photon field in BL Lac is not very clear, which may be caused by the weaker BLR or torus still exist in BL Lacs. Normally, BL Lac show no or very weak emission-line features due to the possible disappearance of BLR. However, some quite weak broad optical emission lines (e.g., Hα, Lyα) are detected in a few BL Lacs (e.g., Corbett et al. 2000; Farina et al. 2012; Fang et al. 2014). In nearby low-luminosity AGNs, it was also found that broad emission lines and torus are still exist but they are much weaker than luminous Seyfert and QSOs (Tran 2001; Gu & Huang 2002; Laor 2003; Elitzur & Ho 2009; Cao 2010; Hönig & Beckert 2007; Ho 2008, e.g.,). The weaker BLR or torus in low-luminosity AGNs or low-power BL Lacs may be caused by (or coevolved with) the transition standard cold disk to radiatively inefficient accretion flows when accretion rate decreases (e.g., Xu, Cao & Wu 2009; Ghisellini & Celotti 2001; Wang et al. 2002; Cao 2003; Wu & Cao 2006). Our results, combined with several former SED modeling of BL Lacs with weak EC components, suggest that BLR or torus may still play a role in Compton scattering in low-power BL Lacs, where BLR/torus may become weak but not fully disappear in these low-power sources (e.g., LLAGNs, FR Is and BL Lacs). Therefore, the seed photon field density (or BLR/torus) may be strongly evolved with possible change of accretion modes from FSRQs to BL Lacs, where the FSRQs and BL Lacs represent the earlier merger-driven phase (gas-rich, efficient accreting) and final phase (gas-starved, inefficiently accreting) respectively (e.g., Ajello et al. 2014).

REFERENCES

Abdo, A. A., et al. 2009, ApJ, 707, 1310A
Abdo, A. A., et al. 2010, ApJ, 716, 30A
Abdo, A. A., et al. 2011a, ApJ, 726, 43A
Abdo, A. A., et al. 2011b, ApJ, 730, 101A
Abramowski, A., Acero, F., Aharonian, F., et al. 2013, A&A, 550, 4
Acciari, V. A., Aliu, E., Arlen, T. et al. 2010, ApJ, 708L, 100A
Acciari, V. A., Aliu, E., Beilicke, M. et al. 2008, ApJ, 684L, 73A
Ackermann, M., Ajello, M., Allafort, A., et al. 2012, Sci, 338, 1190
Ajello, M., Romani, R. W., Gasparrini, D. et al. 2014, ApJ, 780, 73A
Aleksić, J., Alvarez, E. A., Antonelli, L. A., et al.2012, A&A, 542, 100A
Aleksić, J. et al. (the MAGIC Collaboration). 2014, A&A, 567, 135A
Aliu, E., Archambault, S., Arlen, T., et al. 2012, ApJ, 755, 118A
Archambault, S., Aune, T., Behera, B., et al. 2014, ApJ, 785L, 16A
Atwood, W. B., Abdo, A. A., Ackermann, M., et al. 2009, ApJ, 697, 1071A
Błażejowski, M., Sikora, M., Moderski, R., et al. 2000, ApJ, 545, 107B
Blumenthal, G. R., & Gould, R. J. 1970, RvMP, 42, 237B
Bonning, E., Urry, C. M., Bailyn, C., et al. 2012, ApJ, 756, 13B
Böttcher, M. 2005, ApJ, 621, 176B
Böttcher, M., & Chiang, J. 2002, ApJ, 581, 127B
Böttcher, M., Mause, H., Schlickeiser, R. 1997, A&A, 324, 395B
Böttcher, M., Reimer, A., Sweeney, K., Prakash, A. 2013, ApJ, 768, 54B
Böttcher, M., Mukherjee, R. and Reimer, A., 2002. ApJ, 581, 143B.
Cao, X. 2003, ApJ, 599, 147C
Cao, X. 2010, ApJ, 724, 855C
Chen, L., Cao, X., Bai, J. M. 2012, ApJ, 748, 119C
Chen, L., & Bai, J. M. 2011, ApJ, 735, 108C
Cleary, K., Lawrence, C. R., Marshall, J. A., Hao, L., Meier, D. 2007, ApJ, 660, 117C
Cohen, J. G., Lawrence, C. R., Blandford, R. D. 2003, ApJ, 583, 67C
Corbett, E. A., Robinson, A., Axon, D. J., et al. 2000, MNRAS, 311, 485C
D'Ammando, F., Antolini, E., Tosti, G., et al. 2013, MNRAS, 431, 2481D
Dermer, C. D., Menon, G. 2009, High Energy Radiation from Black Holes, Princeton Univerisity Press
Dermer, C. D., & Schlickeiser, R. 1993, ApJ, 416, 458D
Domínguez, A., Primack, J., Rosario, D. J., et al. 2011, MNRAS, 410, 2556D
Dwek, E., & Krennrich, F. 2005, ApJ, 618, 657D
Elitzur, M. & Ho, L. C. 2009, ApJ, 701, 91E
Fang, T., Danforth, C. W., Buote, D. A., et al. 2014, ApJ, 795, 57F
Fanti, C., Fanti, R., Ficarra, A., et al. 1974, A&AS, 18, 147F
Farina, E. P., Decarli, R., Falomo, R., et al. 2012, MNRAS, 424, 393F
Filippenko, A. V., Li, W. D., Treffers, R. R., et al. 2001 ASPC, 246, 121F
Finke, J. D., Dermer, C. D., Böttcher, M. 2008, ApJ, 686, 181F
Finke, J. D., & Dermer, C. D. 2012, ApJ, 751, 65F
Finke, J., Razzaque, S., Dermer, C. 2010, ApJ, 712, 238F
Fleming, T. A., Green, R. F., Jannuzi, B. T., et al. 1993, AJ, 106, 1729F

Franceschini, A., Rodighiero, G., & Vaccari, M. 2008, A&A, 487, 837F

Furniss, A.; Williams, D. A.; Danforth, C.; et al. 2013,ApJ, 768L, 31F

Ghisellini, G., & Celotti, A. 2001, A&A, 379, 1G

Ghisellini, G., Celotti, A., Fossati, G., et al. 1998, MNRAS, 301, 451G

Ghisellini, G., & Madau, P. 1996, MNRAS, 280, 67G

Ghisellini, G., & Maraschi, L. 1989, ApJ, 340, 181G

Ghisellini, G., & Tavecchio, F. 2008, MNRAS, 387, 1669G

Ghisellini, G., & Tavecchio, F. 2009, MNRAS, 397, 985G

Ghisellini, G., Tavecchio, F., Foschini, L., et al. 2010, MNRAS, 402, 497G

Ghisellini, G., Tavecchio, F., Maraschi, L., et al. 2014, Nature, 515, 376G

Gilmore, R.C., Somerville, R.S., Primack, J.R., et al. 2012, MNRAS, 422, 3189G

Giommi, P., Polenta, G., Lähteenmäki, A. et al. 2012, A&A, 541A, 160G

Grauer, A. D., Neely, A. W., & Lacy, C. H. S. 2008, PASP, 120, 992G

Gu, Q., & Huang, J. 2002, ApJ, 579, 205G

Hanski, M., Takalo, L. O., Valtaoja, E. 2002, A&A, 394, 17H

Ho, L. C. 2008, ARA&A, 46, 475H

Hönig, S. F. & Beckert, T. 2007, MNRAS, 380, 1172H

Impey, C. D., & Tapia, S. 1988, ApJ, 333, 666I

Inoue, S. & Takahara, F. 1996, ApJ, 463, 555I

Kang, S. J., Chen, L., Wu, Q. 2014, ApJS, 215, 5K

Kardashev, N. S. 1962, SvA, 6, 317K

Kirk, J. G., Rieger, F. M., Mastichiadis, A. 1998, A&A, 333, 452K

Kneiske, T. M., & Dole, H. 2010, A&A, 515, 19

Kneiske, T. M., Bretz, T., Mannheim, K., et al. 2004, A&A, 413, 807K

Konigl, A. 1981, ApJ, 243, 700K

Krawczynski, H., et al. 2004, ApJ, 601, 151K

Laor, A. 2003, ApJ, 590, 86L

Liao, N. H.; Bai, J. M.; Liu, H. T., et al. 2013, arXiv: 1312.4829L

Liao, N. H.; Bai, J. M.; Liu, H. T., et al. 2014, ApJ, 783, 83L

Lister, M. L., Aller, M., Aller, H., et al. 2011, ApJ, 742, 27L

Maraschi, L.,& Tavecchio, F. 2003, ApJ, 593, 667M

Marscher, A. P., & Gear, W. K. 1985, ApJ, 298, 114M

Mastichiadis, A., & Kirk, J. G. 1997, AAP, 320, 19M

Mirzoyan, R. 2014, ATel, 6349, 1M

Moderski, R., Sikora, M., Coppi, P. S., et al. 2005, MNRAS, 363, 954M

Mankuzhiyil, N., Ansoldi, S., Persic, M., et al. 2011, ApJ, 733, 14M

Mirzoyan, R. 2015, ATel, 7416, 1M

Nieppola, E., Tornikoski, M.,& Valtaoja, E. 2006, A&A, 445, 441N

Ong, R.(the VERITAS Collaboration). 2009, ATel, 2084, 1O

Orienti, M., Koyama, S., D'Ammando, F., et al. 2013, MNRAS, 428, 2418O

Padovani, P.,& Giommi, P. 1996, MNRAS, 279, 526P

Prandini, E.; Becerra-Gonz lez, J.; Lindfors, E., et al. 2012, AIPC, 1505, 647P

Rani, B., Krichbaum, T. P., Fuhrmann, L., et al. 2013, A&A, 552, 11R

Rybicki, G. B., & Lightman, A. P. 1979, Radiative Processes in Astrophysics (New York: Wiley-Interscience), 393

Rovero, A. C., Muriel, H., Donzelli, C., Pichel, A. 2016, A&A, 589, 92R

Sambruna, R. M., Ghisellini, G., Hooper, E., et al. 1999, ApJ, 515, 140S

Shaw, M. S., Romani, R. W., Cotter, G., et al. 2012, ApJ, 748, 49S

Sikora, M., Begelman, M. C., Rees, M. J. 1994, ApJ, 421, 153S

Sikora, M., Moderski, R., Madejski, G. 2008, ApJ, 675, 71S

Sitarek, J., Becerra, G J., Dominis Prester, D., et al. 2015, arXiv: 1508.04580S

Stocke J. T., Danforth C. W., & Perlman E. S. 2011, ApJ, 732, 113S

Teshima, M.(the MAGIC collaboration). 2009. ATel, 2098, 1T

Tornikoski, M., Valtaoja, E., Terasranta, H., et al. 1994, A&A, 289, 673T

Tran, H. D. 2001, ApJ, 554, L19

Urry, C. M., & Padovani, P. 1995, PASP, 107, 803U

Urry, C. M. 1998, AdSpR, 21, 89U

Wang, J.-M., Staubert, R., Ho, L. C. 2002, ApJ, 579, 554W

Wehrle, A. E., Marscher, A. P., Jorstad, S. G., et al. 2012, ApJ, 758, 72W

Wu, Q., & Cao, X. 2006, PASP, 118, 1098W

Xu, Y.-D., Cao, X., & Wu, Q. 2009, ApJ, 694, 107X

Yan, D., Zeng, H., & Zhang, L. 2014, MNRAS, 439, 2933Y

Yan, D., Kalashev, O., Zhang, L., et al. 2015, MNRAS, 449, 1018Y

Yan, D. & Zhang, L. 2015, MNRAS, 447, 2810Y

Zhang, J., Liang, E. W., Zhang, S. N., et al. 2012, ApJ, 752, 157Z

Zhang, J., Sun, X. N., Liang, E. W., et al. 2014, ApJ, 788, 104Z

Zheng, Y. G., & Zhang, L. 2011, ApJ, 728, 105Z

Zheng, Y. G., & Kang, T. 2013, ApJ, 764, 113Z

Zheng, Y. G., Zhang, L., Huang, B. R., Kang, S. J. 2013, MNRAS, 431, 2356Z

Zheng, Y. G., Kang, S. J., Li, J. 2014, MNRAS, 442, 3166Z